

LAL (ORSAY) RF GUN SIMULATIONS AND MODEL CAVITY DESIGN

C. Travier, J. Gao and H. Liu
 Laboratoire de l'Accélérateur Linéaire
 Bât. 200, Centre d'Orsay
 91405 ORSAY Cedex, FRANCE

Abstract

The use of dispenser cathode for RF gun allows both thermionic and laser-driven operation. Simulations results for both cases and cavity design are presented. The status of the project is described.

Introduction

Over the last 5 years, a growing interest for very bright electron sources has been shown in different laboratories around the world. RF gun first developed in Stanford [1] and Los Alamos [2] has the potential of providing such very bright beams. More than twenty RF gun projects are now going on [3], in view of FEL and future accelerators.

At LAL Orsay, we are planning to develop a laser-driven RF gun [4], in order to gain some experience in this field and to provide a possible bright source for the high-gradient accelerator facility NEPAL [5]. A (W, Ba, Ca) dispenser cathode will be used, therefore allowing both thermionic and laser-driven operation [6]. Simulations for both operating conditions are presented here.

A low-level RF model cavity was launched to check some RF properties of the design and to evaluate the size of the coupling slots. Basic design characteristics are presented.

Laser-Driven Gun Simulations

The theoretical investigations that led to the chosen field profile shown in figure 1 are presented in reference 7.

For the simulations done with PARMELA [8] and PRIAM [9], the following assumptions are made. Since the bunch is quite long and the current not too high, the mesh grid method for space charge calculations is preferred to the point to point method [10] in order to save computer time. The effect of image charges in the cathode plane or cavity walls is not included. Electrons are assumed to leave the cathode with no energy and a zero emittance. The laser pulse is taken uniform in both transverse and longitudinal dimensions.

The PARMELA longitudinal random particle generation is changed to a deterministic one. This new generation gives consistent results for 100 particles as compared to 300 to 400 particles needed in the case of the random generation.

The emittance is taken as the normalized r.m.s. emittance defined as $\epsilon_N = 4 \pi \sqrt{\langle x^2 \rangle \langle (p_x/mc)^2 \rangle - \langle x(p_x/mc) \rangle^2}^{1/2}$ where x is the coordinate of a particle in the beam, p_x is the particle's momentum component in the x direction and $\langle \rangle$ indicates averaging over the entire beam. It corresponds to the "90 % emittance" for a beam which distribution is gaussian in each coordinate.

The optimization procedure and the results for different values of accelerating field are given in reference 4. Results are presented here for a maximum on-axis field of 70 MV/m corresponding to a maximum surface field of 112 MV/m which is just above two times the Kilpatrick limit. 30 ps laser pulse length is assumed. Figures 2 and

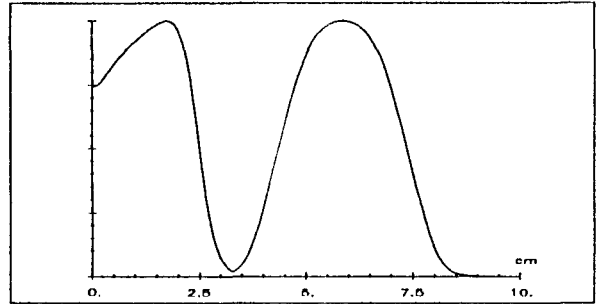


Fig. 1: Longitudinal on-axis electric field

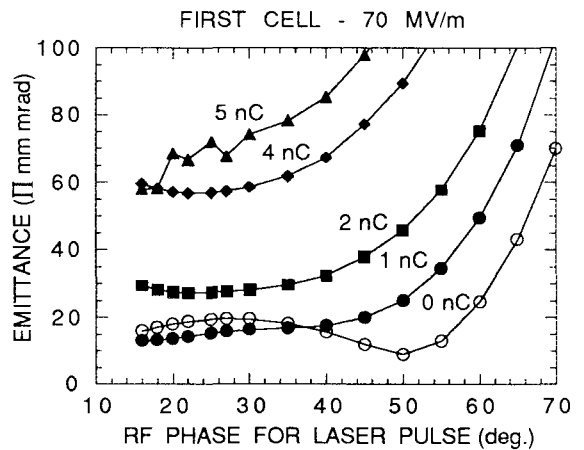


Fig. 2: Emittance vs. laser phase after first cell

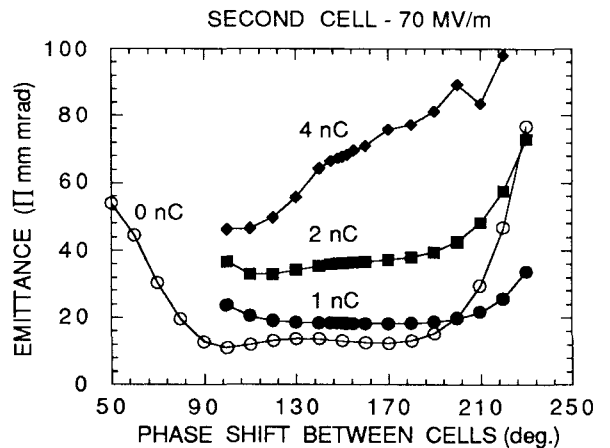


Fig. 3: Emittance vs. ϕ_{12} after second cell

3 show the emittance as function of the RF phase for laser pulse at the end of the two cells for different values of the bunch charge. For 4 nC, some particles are lost within the second cell, while for 5 nC, some are lost in the first cell. Table 1 gives the main parameters for a typical run.

Thermionic Gun Simulations

When running the gun in a thermionic way, the goal is to provide an electron beam to test the various measurement devices.

Since, in this case, the electron micropulse repetition rate is high, the cathode should work at a low temperature to limit the extracted current, in order to limit the beam loading. On the other hand, we should have an output energy roughly as high as for the laser-driven case. Based on these considerations, we have investigated the gun performances.

The thermionic emission of electron micropulses is assumed to obey the Richardson-Schottky equation. For a typical case, one has $T = 1000$ K, $\phi_0 = 1.9$ eV, $\bar{E}_1 = \bar{E}_2 = 35$ MV/m and $\phi_{12} = 156.5^\circ$, where T and ϕ_0 represent the operating temperature and work function of the cathode, respectively; \bar{E}_1 and \bar{E}_2 represent the average on-axis electric field amplitudes in each cell; ϕ_{12} is the phase shift between the two cells. In this case, the beam loading is around 0.2 MW. The characteristics of the electron micropulse out of the second cell are shown in figure 4.

A transport line similar to that of BNL [11] is considered. Based on the beam parameters at the exit of the second cell obtained with PARMELA, the transport line parameters are calculated with TRANSPORT [12]. Then the beam dynamics along such a transport line is simulated again using PARMELA. The first results show that the normalized r.m.s. emittances are increased finally to about 20π mm mrad for x dimension and to about 12π mm mrad for y dimension, from an initial value of 6π mm mrad for both dimensions; for such a case, the total energy spread and phase spread are 36 keV and 7° respectively, with the central energy at 2.866 MeV; the r.m.s. energy spread and r.m.s. phase spread are 9 keV and 2° respectively; the average current is about 4 mA. These values correspond to a small fraction of the beam that could be selected with momentum slits.

Cavity Design

The cavity design constraints are as follows: obtain a field profile as close as possible to the theoretical one, minimize the peak surface field, obtain decoupled cells separated by the shortest drift possible and with the lowest priority, maximize the shunt impedance. The cavity which contour is shown in figure 5 is designed with SUPERFISH [13]. Figure 6 shows a PRIAM 3-D view of the cavity as provided by G. Le Meur. Table 2 gives the RF parameters as obtained with SUPERFISH, PRIAM and MAFIA [14] codes. Following the work done in references 15 and 16, MAFIA calculations of the coupling slots size were performed: the results are shown in figure 7. Figure 8 shows a 3-D EUCLID [17] view of the model cavity recently manufactured. This model cavity will be used to check that the cells are decoupled, to determine the coupling slots size, to estimate the unsymmetrical field distortion due to these coupling slots and to check the efficiency of the $\lambda/2$ stub used for the cathode holder. Measurements will proceed soon.

Project Status

Simulations are continuing for both the laser driven and thermionic cases. Different parameters will be investigated. A two stage experiment is foreseen. First, the gun itself will be tested in both operating modes. At

Table 1: Parameters for a typical run

Laser pulse length (ps)	30.	
Laser spot radius (mm)	3.	
RF Frequency (GHz)	3.	
First cell length (cm)	3.325	
Second cell length (cm)	5.835	
Cell aperture radius (mm)	5.	
Emittance at cathode (π mm mrad)	0.	
Magnetic field (T)	0.	
Number of particles	100	
Charge in a bunch (nC)	2.	
RF phase for laser pulse (deg.)	22.	
Phase shift between cells (deg.)	150.	
	1 st cell	2 nd cell
Max. electric field (MV/m)	70.	70.
Kinetic energy (MeV)	1.326	2.867
Bunch length (ps)	17.	17.
Peak current (A)	118.	118.
Bunch radius (r_{max}) (mm)	3.1	3.9
Max. energy spread (keV)	186.	33.
Max. energy spread (%)	14	1.1
Emittance (π mm mrad)	27.3	34.2
Emittance (RF) (π mm mrad)	18.7	15.5
Angular divergence (mrad)	44.7	24.2

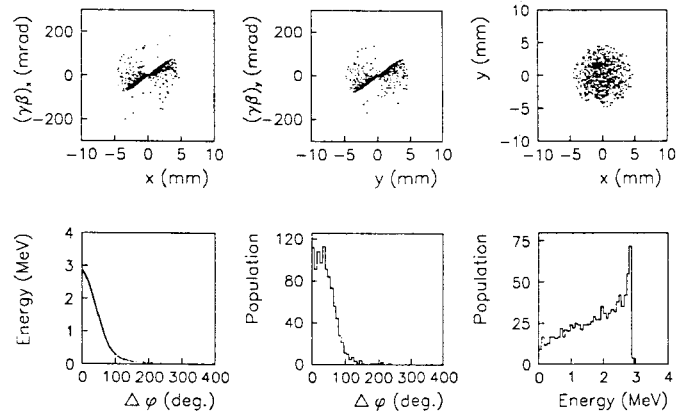


Fig. 4: Thermionic gun simulation

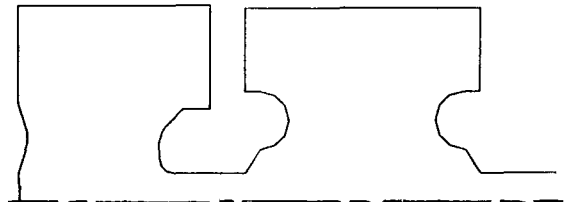


Fig. 5: Cavity contour (upper-half)

this stage, it will be followed by a transport line including measurement devices that could be either an "α-magnet" or a line similar to that of BNL [11]. At a second stage, it is planned to place the gun directly upstream from a high gradient accelerating structure. This small accelerator will then be followed by a magnetic bunching system. This configuration will allow us to experiment the method described by B. Carlsten [18] to reduce emittance. Simulations for this second stage of experiment will be performed very soon. A low-level RF model cavity was built. Measurements will start soon. The final prototype design should be completed by the end of 1990. The first beam is scheduled for the first semester of 1991.

Acknowledgements

We would like to thank Y. Thiery who performed all the lengthy simulation runs for the laser-driven case and B. Mouton who diligently modified PARMELA according to our wishes. We greatly appreciated the help of G. Le Meur when using PRIAM. We are pleased to thank H. Hanaki who performed the MAFIA calculations. M. Desmons is acknowledged for the mechanical design of the cavity. Many valuable advices from several colleagues were greatly appreciated. Finally, we wish to thank Dr. J. Le Duff for his constant support.

References

- [1] G.A. Westenskow, J.M.J. Madey, Laser and Particle Beams (1984), Vol 2, Part 2, pp. 223-225.
- [2] R.L. Sheffield et al., Proc. of the 1988 Linear Acc. Conf., Williamsburg, VA, October 3-7, 1988, pp. 520-522.
- [3] C. Travier, Proc. of the Workshop on Short Pulse High Current Cathodes, Bendor, France, June 18-22, 1990.
- [4] C. Travier, J. Gao, Proc. of the 2nd European Part. Acc. Conf., Nice, June 12-16, 1990.
- [5] G. Bienvenu, Proc. of the 2nd European Part. Acc. Conf., Nice, June 12-16, 1990.
- [6] H. Bergeret, M. Boussoukaya, R. Chehab, B. Leblond, J. LeDuff, Proc. of the Workshop on Short Pulse High Current Cathodes, Bendor, France, June 18-22, 1990.
- [7] J. Gao, to be published in the Proc. of the 12th FEL Conf., Paris, Sept. 17-21, 1990.
- [8] Version from K. Crandall and L. Young at LANL, with modifications from K.T. McDonald (BNL), B. Mouton (LAL) and H. Liu (IHEPB). User's manual from B. Mouton, LAL/SERA 89-356, 1989.
- [9] G. Le Meur, Proc. of the 2nd European Part. Acc. Conf., Nice, June 12-16, 1990.
- [10] K.T. McDonald, DOE/ER/3072-43, Princeton University, 1988.
- [11] X.J. Wang et al., Proc. of the 1989 Part. Acc. Conf., Chicago, March 1989, p. 307.
- [12] K.L. Brown et al., CERN 80-04, SPS Division, 1980.
- [13] K. Halbach, R.F. Holsinger, Proc. of the 1976 Part. Acc. Conf., pp. 213-222
- [14] e.g.: G. Fischerauer, T. Weiland, Proc. of the 2nd European Part. Acc. Conf., Nice, June 12-16, 1990.
- [15] T.F. Wang et al., Proc. of the 1988 Linear Acc. Conf., Williamsburg VA, October 3-7, 1988, p. 373.
- [16] H. Henke, W. Wuensch, CLIC note 108, 1990.
- [17] 3-D mechanical design code from MATRA Datadivision.
- [18] B.E. Carlsten, R.L. Sheffield, Proc. of the 1988 Linear Acc. Conf., Williamsburg VA, October 3-7, 1988, pp. 365-369.

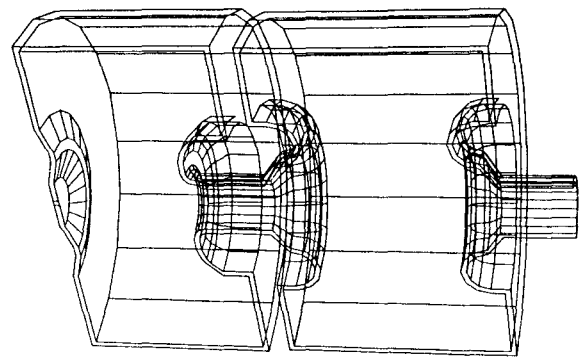


Fig. 6: PRIAM view of the cavity

Table 2: Cavity RF parameters

	1 st cell	2 nd cell
SUPERFISH (2-D)		
Frequency (MHz)	2993.8	2990.8
Shunt impedance Z ₀ (MΩ)	3.26	3.39
Quality factor	11880	11353
Field ratio*	1.61	1.54
Mesh size (mm)	0.5	0.6
PRIAM (2-D)		
Frequency (MHz)	2989.5	2989.0
Field ratio*	1.3	1.3
Mesh size (mm)	1.-2.	1-1.5
MAFIA (3-D)		
Frequency (MHz)	2881.95	2832.3
Shunt impedance Z ₀ (MΩ)	3.17	3.
Quality factor	11610	10420
Field ratio*	1.46	1.36
Mesh size (mm)	0.75-4.	0.6-2.5

*: Max. surface field / max. on-axis field

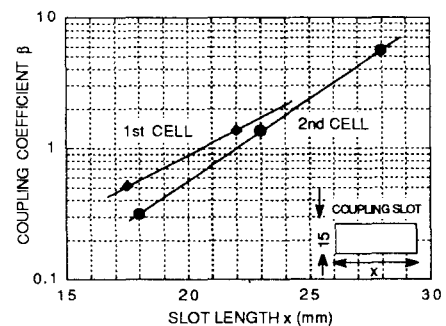


Fig. 7: MAFIA calculation of coupling slots

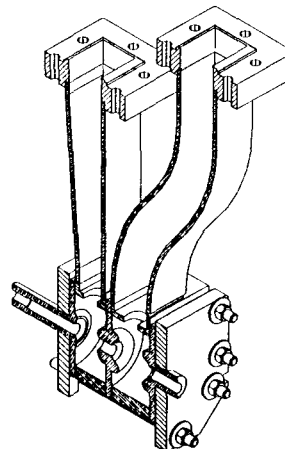


Fig. 8: EUCLID view of the model cavity